

# MEASUREMENT AND MODELING OF NIP ROLLER FEED RATES

BY

KEVIN COLE, PhD  
Senior Web Handling Development Engineer  
Optimation Technology Incorporated

## Introduction

Nip rollers are used extensively in converting processes; however, elastomeric-covered rollers have the unwanted and often unpredictable characteristic of unknown surface speed owing to coupling between circumferential and radial strains within the nip. In this paper, a measurement method is described and demonstrated for accurately measuring nip roller feed rates. Modeling techniques are also presented for predicting nip roller feed rate and results compared to experimental data. A novel contribution of this paper is the demonstration of the ability to analyze roller coverings engineered with the ability to control nip roller feed rate while retaining nip pressure characteristics. This is an important capability in light of the known negative influence of non-uniform nip roller feed rate due to cross-direction variations on web troughing and wrinkling propensity.

## Nip Mechanics Overview

When webs are conveyed by elastomeric-covered nip rollers, it is often the case that the speed of the web is different from the nominal surface speed of the rollers away from the nip (see Stack et. al. [1995]). This behavior is influenced by a number of factors, including the physical properties of the elastomeric coverings, geometric characteristics such as cover thicknesses and roller diameters and process conditions such as the engagement of the rollers and tension difference in the web across the nip rollers. Owing to this behavior, nip systems are often comprised of one elastomeric covered roller and one roller without an elastomeric covering. The web is typically wrapped over the uncovered roller and if the nip roller pair is a drive, the uncovered roller is usually driven. This being said, deleterious effects due to the inherent tendency of the elastomeric-covered roller to travel at a different nominal surface speed compared to the web speed can still be present. Two examples are: (a) small relative motion (e.g., micro-creep) in the machine direction leading to the potential for abrasions and dirt generation and (b) differential relative motion in the transverse direction leading to an increased risk of the formation of unwanted lateral tracking and wrinkling. Transverse direction effects can arise due to differing amounts of roller engagement due to roller core bending effects. This follows from the fact that the differential surface speed is a function of roller engagement.

Figure 1 shows a cross sectional view of an elastomeric roller (number 1) loaded against an uncovered backing roller (number 2). No web is considered to be in the system. Prior to contact,

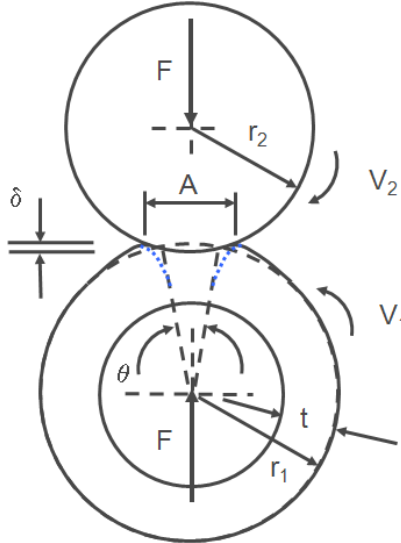


Figure 1: Nip roller system cross-sectional view

each particle on the surface of each roller rotates at the same surface speed,  $V$ . Assuming roller 2 to be driven, it will still travel at the same surface speed after the rollers are brought into engagement by an amount,  $\delta$ . Therefore,  $V_2 = V$ . However,  $V_1$  will no longer be equal to  $V$ . To determine  $V_1$ , it is noted that the characteristics of the elastomeric covering on roller 1 determine the circumferential strain that develops within the contact, or nip, zone. The angle,  $\theta$ , is defined as the angle subtended by the nip zone in roller 1 assuming that there is no circumferential strain in the cover. Under this assumption, the nip width is equal to  $r_1\theta$  and the interval of time required for roller 1 to rotate through this angle is found from the following:

$$\Delta t = r_1\theta / V_1 \quad (1)$$

Owing to the coupling between radial and circumferential strains, the actual nip width,  $A$ , will be different than the theoretical nip width by some nominal amount,  $\epsilon$ , which we refer to as the creep of the system:

$$A = (1 + \epsilon)r_1\theta \quad (2)$$

The creep is the average circumferential strain in the nip zone which, as we shall next show, relates to the speed of roller 1. Owing to mass conservation, a particle on the surface of roller 2 must travel through the actual nip in the same interval of time as roller 1 rotates through  $\theta$ .

$$\Delta t = A/V_2 = A/V \quad (3)$$

Combining equations (1) through (3) yields the surface velocity of roller 1 in terms of the creep:

$$V_1 = V / (1 + \varepsilon) \quad (4)$$

Equation (4) indicates that for positive creep, the elastomeric-covered roller will travel at a slower speed than the drive roller and that for negative creep, the elastomeric-covered roller will travel at a higher speed than the drive roller.

For linear elastic materials, there are two material constitutive properties that influence the relationships between deflections, loads and creep within a system such as shown in Figure 1. The first, Young's modulus,  $E$ , is roughly a measure of radial stiffness and the second, Poisson's ratio,  $\nu$ , is a measure of compressibility.

Reference 2 (Good [2001]) provides detailed information about both of these properties. In that work, it was shown that for natural and synthetic rubbers, Shore A (i.e., IRHD) hardness measured with a hand-held instrument is adequate to predict Young's modulus. The relationship between Shore A hardness and modulus was found to be given by the following expression (reference 2, equation 1):

$$E_o = 20.97e^{0.0564*IRHD} \text{ (psi)} \quad (5)$$

where the subscript indicates modulus excluding confinement effects. Suitable modifications to account for confinement in the nip zone are provided (reference 2, equation 5).

For linear elastic materials, a value of Poisson's ratio approaching 0.5 corresponds to an incompressible material. Materials such as polyurethanes and rubbers have a Poisson's ratio approaching 0.5. Owing to the incompressible nature of these types of typical roller coverings, radial strains due to roller engagement leads to significant positive circumferential strain resulting in positive values of creep. Reference 2 reports that a value of 0.46 seems to be valid over a wide range of durometers and elastomeric materials. We will use this value in the work that follows.

At the other extreme, open cell foams have a Poisson's ratio approaching 0. In this case, creep may actually be negative resulting in a roller covered with such a material going faster than the driven roller. One such case will be examined in the work that follows.

## Nip Deflection/Nip Roller Feed Rate Models

Reference 2 (Good [2001]) provides a description of several nip deflection models relating nip width to roller engagement or deflection. The most useful of these models is that proposed by Johnson (reference 2, equation 18):

$$F = \frac{2(1-\nu)^2}{3} \frac{E_0}{1-2\nu} \frac{\sqrt{2R}}{1-\nu^2} \frac{\delta^{3/2}}{t} \quad (6)$$

where  $\nu$  is Poisson's ratio,  $R$  is the equivalent radius (which for a pair of rollers shown in Figure 1 can be written as  $R=(R_1R_2)/(R_1+R_2)$ ),  $t$  is the cover thickness on roller 1, and  $\delta$  is the engagement of the two rollers. A corrected version of equation 6 accounting for rubber confinement in the nip zone is provided by equation 27 in reference 2.

Unfortunately, the model provided by equation (6) does not predict creep. For that purpose, another model (referred to as the Cole model) has been developed that predicts creep in addition to load/deflection and nip width/load. The load/deflection results from this model will be compared to equation (6) and the creep predictions will be compared to experimental data collected using a method that is described in the next section.

A brief overview of this model will now be provided. Additional details can be provided at the request of the author. Reference 3 (Timoshenko [1970]) likewise provides a discussion of this solution method. The derivation of the model begins by the development of a closed form analytical solution to the problem of stresses and strains within a finite thickness layer of linear elastic material. The solution is exact with the assumption that the loading and displacements are sinusoidal. The layer is infinite in length (corresponding to the circumferential direction of the elastomeric cover) and of unit thickness in depth (corresponding to the axial direction in the elastomeric cover). Figure 2 shows a cross section of the finite layer of thickness  $t$  with sinusoidal loading at the bottom and top of the layer. Plain strain is assumed for the layer. This is consistent with the constraint experienced by a typical elastomeric coating which typically is wider than the nip width or thickness.

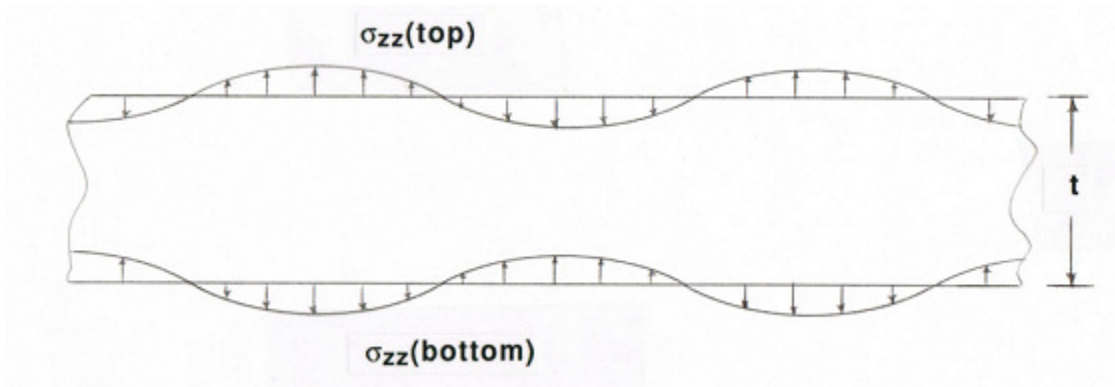


Figure 2: Nip roller elastomeric cover cross-sectional view

Fourier series expansion is then used to solve for the response at one point along the surface of the strip due to a load at another point. To facilitate the derivation, the interpolation function,  $\text{sinc}(x)=\sin(x)/x$ , where  $x$  is the coordinate along the length of the strip. This function has the desirable characteristic of equaling 1 at the load application point and zero at all other equally spaced points away from the load point. The response of the strip to this interpolation function can be found by means of a Fourier integral over a finite frequency range since the *Sinc* function has the further desirable characteristic of having a finite frequency spectrum.

Figure 3 shows a sketch of the content of an arbitrary loading distribution. The figure also illustrates that the layer can be subdivided into more than one layer. This provides the capability to model elastomeric covered rollers with multiple sublayers. The model currently can handle up to 8 sublayers, each with arbitrary thickness, Young's modulus and Poisson's ratio.

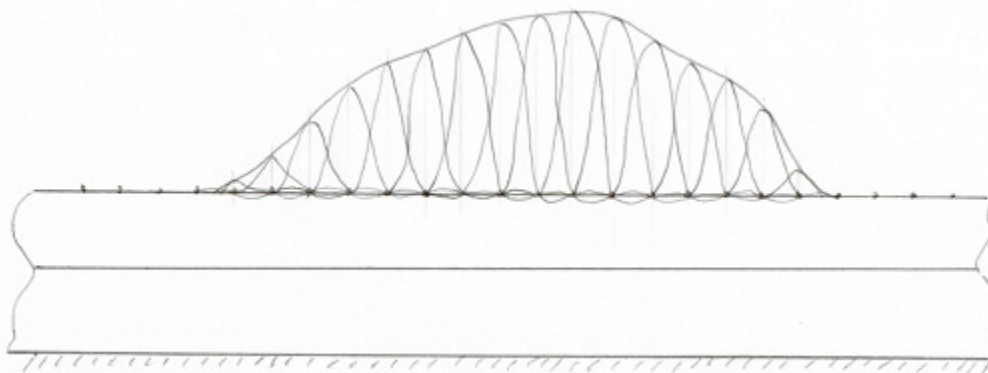


Figure 3: Elastomeric cover general loading, multiple layers

Application of the general strip solution to the nip roller pair shown in Figure 1 is made by writing geometric compatibility equations accounting for the cylindrical geometry of the rollers. For a specified roller engagement, the displacement within the nip is known and outside of the nip, the normal stress is equal to zero. The nip width, which initially is unknown, is found by iteration until the boundary conditions inside and outside of the nip zone are satisfied. Once a solution is found, the circumferential creep is computed by averaging the lengthwise strains in the nip zone.

Figures 4 through 6 show a comparison results from the KL Johnson model (equation 6), the Cole model and experimental data obtained from the Thin Web Rewinder (TWR) in the Optimization Media Conveyance Facility. In the next section, the method used to obtain the experimental results will be described. The results are for a nip roller pair with the following characteristics (refer to Figure 1 for geometry): roller #1 radius = 3.005 inch, elastomeric cover thickness (one layer) = 0.375 inch, elastomer cover durometer = 50 Shore A, elastomer cover Poisson's ratio = 0.46, and roller #2 radius = 6.3095 inch.

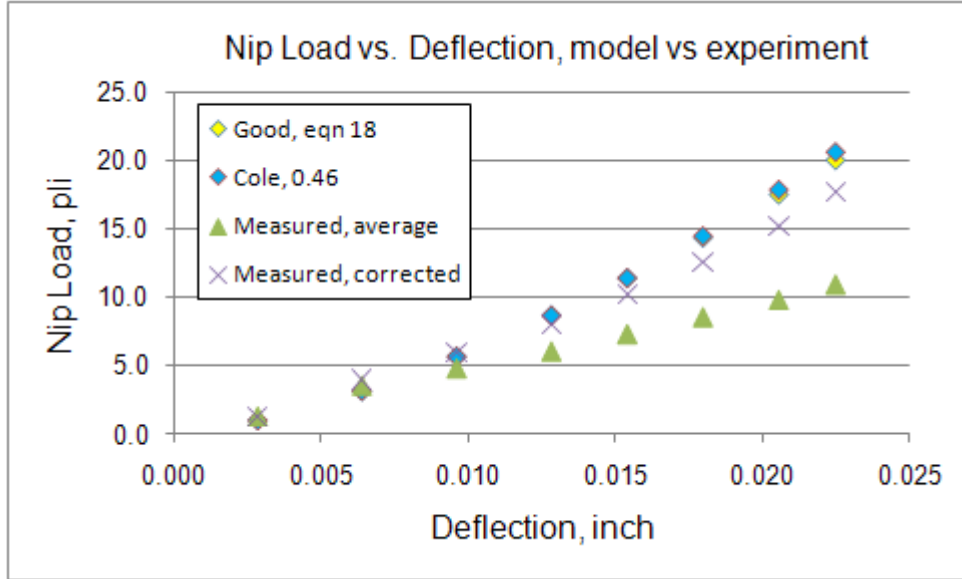


Figure 4: Nip Load versus Roller Deflection, baseline case

Figure 4 shows good agreement between the two models. The measured data, however, does not agree well with the theoretical data. The reason for the discrepancy was determined to be due to the fact that the deflection was measured at the end of the roller where the nip load was greater than the nominal nip load across the width of the roller. Correcting for this difference yielded results in better agreement with theory.

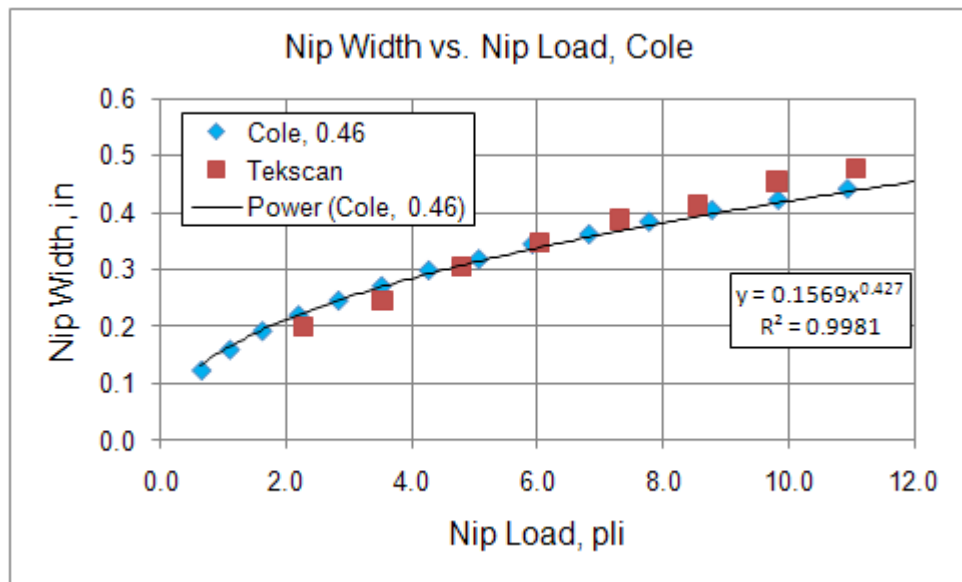


Figure 5: Nip Width versus Nip Load, baseline case

Excellent agreement is seen between theory (Cole) and the measured nip width versus nip load. The measured nip width is the average value over four measurements across the width of the roller.

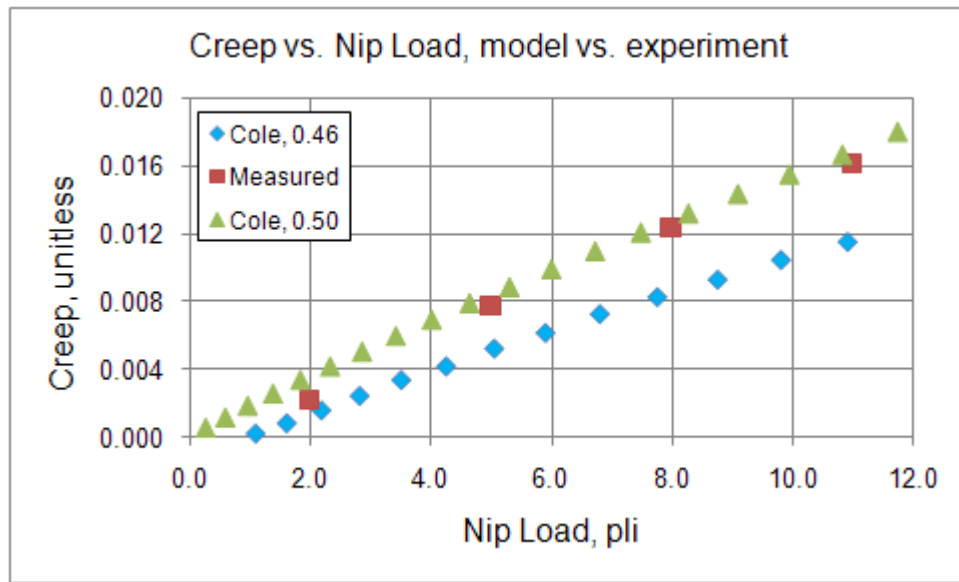


Figure 6: Creep versus Nip Load, baseline case

Creep is plotted in Figure 6. For positive creep, the elastomeric covered roller rotates at a reduced speed. This result is expected for a single layer of very nearly incompressible material. The agreement between theory and experiment is not as good as the previous predictions and perhaps reflects the effect of neglecting friction in the nip zone. However, small changes in Poisson’s ratio near 0.5 will have a rather large effect on predictions of creep. The curve for Poisson’s ratio equals to 0.5 is also shown in Figure 6 and the agreement between experiment and prediction is excellent at this higher value of Poisson’s ratio.

So which value of Poisson’s ratio should be used? Based on the overall agreement between the experimental data, the value of 0.46 gives the best overall agreement between load/deflection and nip width/nip load while the value of 0.50 gives the best agreement between creep/nip load. Owing to the assumptions used to compute creep (no friction, average of the strain within the nip zone), it is believed that a stronger weighting needs to be given to the load/deflection/nip width data. Therefore, 0.46 is used in the results which follow (as per reference 2).

### Measurement of Load/Deflection and Creep

Experiments were conducted in the Media Conveyance Facility to obtain experimental data to verify the models described in the previous section. For that purpose, a nip roller module duplicating the configuration shown in Figure 1 was constructed on the TWR. A picture of the module is shown in Figure 7. The configuration consists of an idling lower uncovered roller and an upper roller with an elastomeric covering. Both are driven at a constant machine speed by

means of a 12 micron PET web wrapped partially around the lower uncovered roller. Nip force is controlled by two air cylinders mounted at either end of the live-shafted elastomeric covered

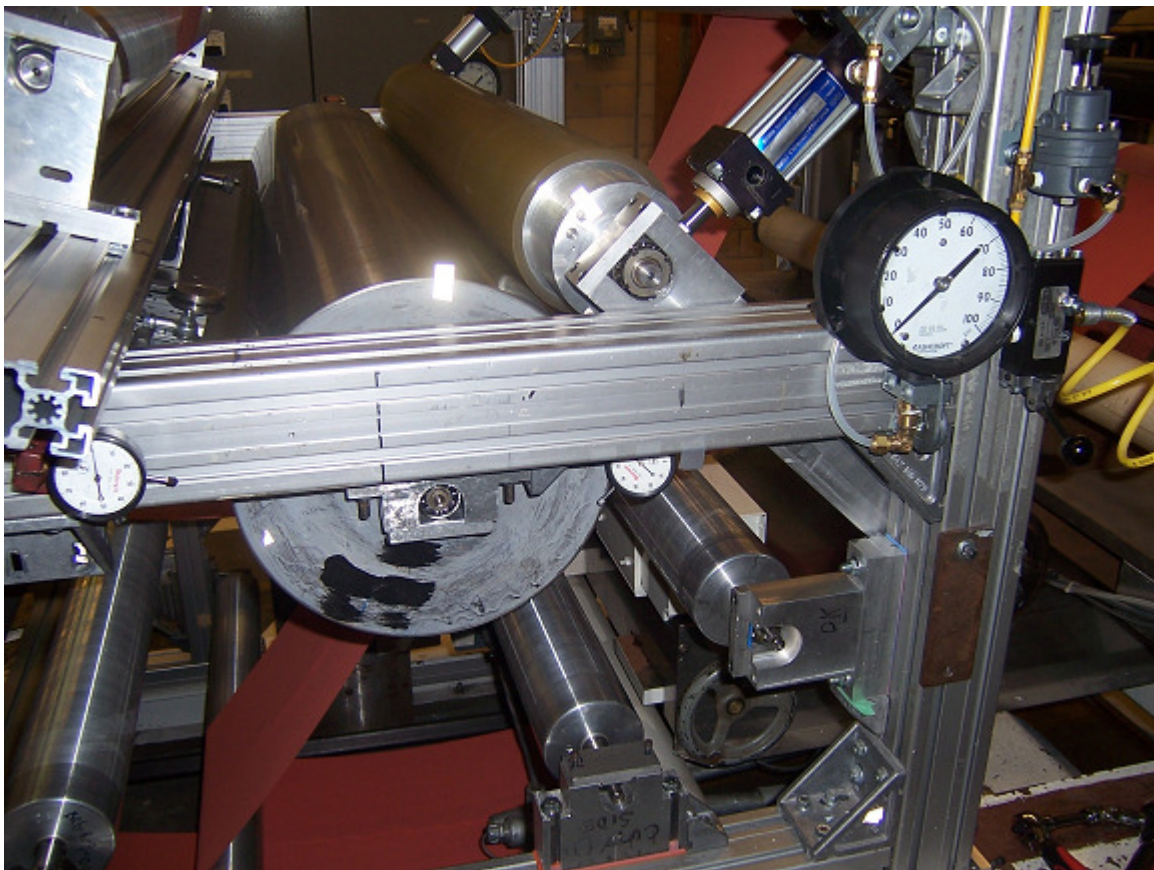


Figure 7: Nip module setup on TWR

nip roller. The nip roller is attached to two pivoting arms which maintain alignment and provide a reference to measure roller engagement using mechanical dial indicators.

Nip width is measured using the Tekscan™ I-Scan measurement system. This system consists of sensors that detect pressure changes as an electrical resistance drop through a conductive ink. In the results presented in the previous section, the nip width was measured at 4 locations across the width of the roller and averaged to give the results shown in Figure 5.

Creep was measured using a “spindown tester”. A spindown tester is an electronic instrument intended for accurately measuring the angular velocity and angular acceleration of a roller. It requires an optical sensor, a spindown tester electronics box, and a standard computer (“PC”) with a serial port. The measurement is accomplished by using a non-contacting optical sensor to provide an electrical voltage signal, or pulse, for each revolution of the roller. The spindown instrument contains a quartz-crystal-controlled master clock that runs at 2,457,600 Hz. This master clock drives a 36-bit counter. Every time a pulse from the sensor is detected, the content

of this counter is latched into a 36-bit register. This register then remembers the count at the time of the pulse for a short while – long enough to transmit the stored 36-bit value to a computer. The computer then remembers the value indefinitely, along with that of all the other revolutions. This has the effect of storing the time of the occurrence of every roller revolution to an accuracy of about 0.4 microseconds.

The 36-bit “times” of every revolution may then be regenerated in the computer and divided by 2,457,600 to give a time in seconds for the occurrence of every roller revolution. One may estimate the roller’s angular velocity by  $v = \frac{2 \cdot \pi}{\Delta t}$  (radians/second), where  $\Delta t$  is the time difference between the start of one roller revolution and the start of the next revolution in seconds. The time at which this velocity is deemed to have occurred is estimated by the average of the start time of the revolution and the start time of the next revolution, and is designated as  $t_v$ . Then the roller’s angular velocity is estimated by  $a = \frac{\Delta v}{\Delta t_v}$  rad/sec<sup>2</sup>. The time at which this acceleration is deemed to have occurred is the average of the two  $\Delta t_v$  values used in the calculation of the acceleration. Velocities and accelerations measured in this fashion exhibit no systemic errors under constant acceleration. They do exhibit a bias error under constant jerk conditions (i.e., a ramp of acceleration).

Creep can be computed from a knowledge of the rotation times for the two rollers according to the following equations:

$$t_1 = 2\pi(1 + \varepsilon)r_1/V \tag{7}$$

and

$$t_2 = 2\pi r_2/V \tag{8}$$

giving:

$$\varepsilon = r_2 t_1 / r_1 t_2 - 1 \tag{9}$$

## Measurement of Dual Durometer Roller Creep

Two additional rollers, provided by American Roller Company, were tested to assess the creep prediction theory. One roller was constructed with a single elastomeric layer ( $r_l = 3.125$  inch,  $t = 0.500$  inch, durometer = 40 Shore A, Poisson’s ratio assumed equal to 0.46) and the second was constructed with a dual layer ( $r_l = 3.3125$  inch,  $t_{inner} = 0.690$  inch,  $t_{outer} = 0.060$  inch, inner layer durometer = unknown, inner layer Poisson’s ratio unknown, outer layer durometer = 60 Shore A, outer layer Poisson’s ratio assumed equal to 0.46). Figures 8 and 9 show the theoretical and

experimental nip width versus nip load and creep versus nip load for the dual durometer roller and the theoretical results only for the single durometer roller. Correlation between the model and experiment required some iteration on the hardness and Poisson's ratio of the lower layer on the dual durometer roller. A value of durometer equal to 5 Shore A and a Poisson's ratio of 0.35 gave the best agreement between the model and predicted results. Interestingly, the dual durometer roller had negative creep indicating that the roller actually traveled faster in the test module during the experiments.

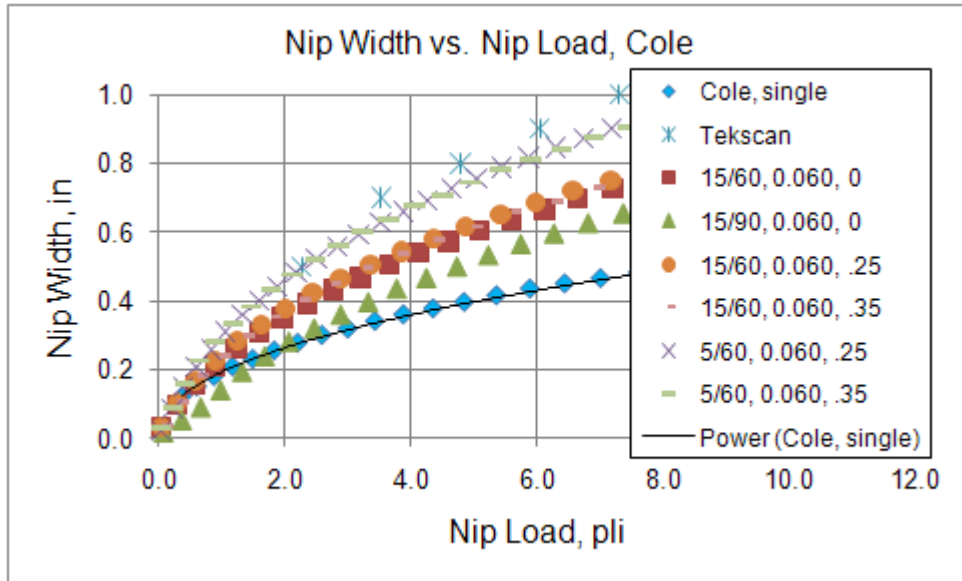


Figure 8: Nip width versus nip load, single/dual durometer nip rollers

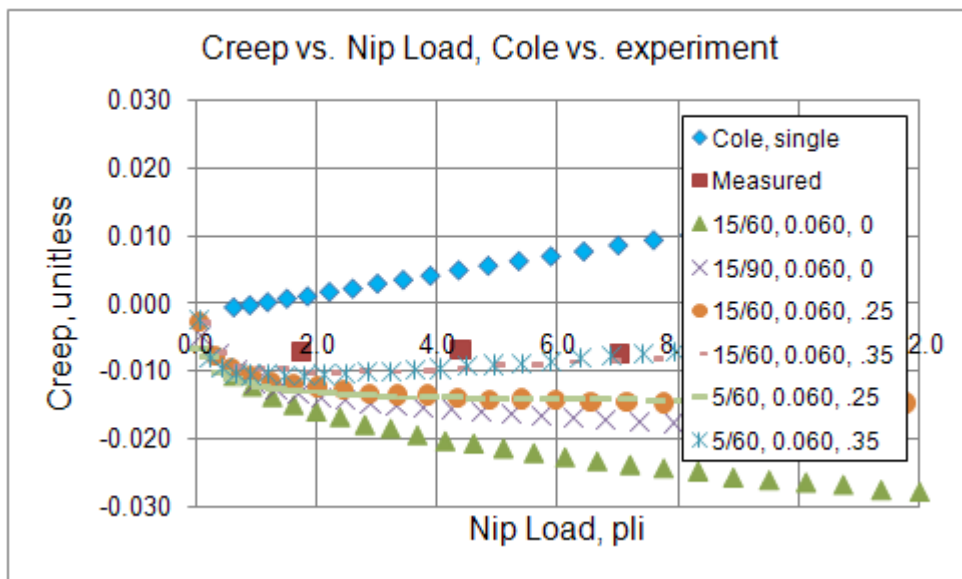


Figure 9: Creep versus nip load, single/dual durometer nip rollers

## Conclusions

A theoretical model predicting creep within a nip roller pair consisting of a uncovered roller nipped against an elastomeric covered roller has been presented. A method for collecting experimental creep data has also been described. Experiments were conducted to collect data to compare to the theoretical model. Results for both a single durometer cover and a dual durometer cover were obtained and compared to model predictions. Good agreement between the model and experiment was demonstrated.

### Acknowledgements:

The author thanks American Roller Company for their contribution of the single and dual durometer pressure roller covering and Tim Walker and Mike Kubiak for their assistance with data collection and analysis.

### References:

1. Stack, K.D., et. al, "The Effects of Nip Parameters on Media Transport", Proceedings of the 3<sup>rd</sup> International Conference on Web Handling, Stillwater, OK, 1995, ed J K Good, pp 382-395.
2. Good, J.K, "Modeling Rubber Covered Nip Rollers in Web Lines", Proceedings of the 6<sup>th</sup> International Conference on Web Handling, Stillwater, OK, 2001, ed J K Good, pp 159-177.
3. Timoshenko, "Theory of Elasticity", McGraw-Hill Book Company, Third Edition, pp 53-60.

### Author Contact Information:

Dr. Kevin Cole  
Senior Web Handling Development Engineer  
Optimation Technology Incorporated  
Rochester, New York 14652-3254  
585-703-0514 (work phone), 585-321-2700 (fax)  
e-mail: kevin.cole@optimation.us